Modeling, Design & Characterization of A Novel Passive Variable Stiffness Joint (pVSJ)

Mohammad I. Awad*[1], *IEEE Student Member*, Dongming Gan[1], *PhD*, Marco Cempini[2], *IEEE Member, PhD*, Mario Cortese[2], *PhD*, Nicola Vitiello[2,3], *PhD*, Jorge Dias[1,4], *IEEE Senior Member, PhD*, Paolo Dario[2] , *IEEE Fellow, PhD* , Lakmal Seneviratne[1,5], *IEEE Member, PhD*

***Abstract*— In this paper we present the design and characterization of a novel Passive Variable Stiffness Joint (pVSJ). pVSJ is the proof of concept of a passive revolute joint with controllable variable stiffness. The current design is intended to be a bench-test for future development towards applications in haptic teleoperation purposed exoskeletons. The main feature of the pVSJ is its capability of varying the stiffness with infinite range based on a simple mechanical system. Moreover, the joint can rotate freely at the zero stiffness case without any limitation. The stiffness varying mechanism consists of two torsional springs, mounted with an offset from the pVSJ rotation center and coupled with the joint shaft by an idle roller. The position of the roller between the pVSJ rotation center and the spring's center is controlled by a linear sliding actuator fitted on the chassis of the joint. The variation of the output stiffness is obtained by changing the distance from the roller-springs contact point to the joint rotation center (effective arm). If this effective arm is null, the stiffness of the joint will be zero. The stiffness increases to reach high stiffness values when the effective arm approaches its maximum value, bringing the roller close to the torsional springs' center. The experimental results matched with the physical-based modeling of the pVSJ in terms of stiffness variation curve, stiffness dependency upon the springs' elasticity, joint deflection and the spring's deflection.**

I. Introduction

The need of robots operating closely to humans either associating, physically interacting, or even worn by them has risen several aspects and design requirements. Although the general aspects of efficiency and robustness are taken with high importance, safety is considered one of those most important aspects. Safety should be able an intrinsic feature in robots especially in the case of unexpected interactions, or sensor failures [1]. Beside the safety aspect, the interaction between the robot and the operator must show adaptability and force accuracy. This aspect has taken its importance in many applications such as rehabilitation robots, exoskeletons and haptics.

The previously mentioned aspects have motivated the development of variable impedance actuators (VIA), of which the actuator mechanical properties (inertia, damping or stiffness) affect the system equilibrium position [2]. This changes the interaction forces to adapt to different situations between the robots and the environment or users to provide safe operations and energy efficiency [2]. Based on how the impedance (stiffness and damping) is achieved, active and passive VIA concepts were proposed. In the active-by-control impedance, the behavior of a highly-reduced stiff actuator is altered via software. This concept was pioneered by DLR and adapted by KUKA [3], and it allows to adapt both stiffness and damping in a wide range and for several speeds. The disadvantages of this system lie in the high energy consumption, the need of very accurate and expensive force/torque sensors, the complexity of the control system, the incapability of storing energy and absorbing shocks [4, 31]. To overcome such drawbacks, passive compliant elements can be added to the actuator. This was early approached in the Serial Elastic Actuator (SEA) [5]. Several techniques on the SEA structures and control systems were presented in the literature [6-10]. The drawbacks of the SEA lie in the non-optimal performance and non-optimal energy efficiency. The optimal performance needs careful tuning of the joint stiffness values [11]. This motivated lots of study and new designs of variable stiffness mechanisms with passive compliance [12].

One of the easiest ways to vary actuator's stiffness is by changing the spring preload. In this type, altering the perceived stiffness is achieved by changing the energy stored in the spring [31]. One evolution of this concept is the antagonistic variable stiffness actuators, where the joint stiffness is varied through the combination of two antagonistic SEAs controlled by two separate motors. Designs which fall into this category include VSA-I [6], VSA-II [13], AMASC [14], and the biological inspired joint stiffness control mechanism [15]. Other techniques were applied and several solutions were presented such as using a nonlinear connector between the output link and the spring element to adjust the preload of the linear spring shown in the MACCEPAs [16-17]. Another principle for stiffness altering is to apply a lever mechanisms between the output link and the elastic element. Varying stiffness is achieved by altering the link length between the pivot and either the elastic element or the output link. Examples of this type include the AwAS [18], AwAS-II [19], CompAct-VSA [20], the vsaUT [21], the mVSA-UT [22], and the vsaUT-II [23].

Mohammad I. Awad is corresponding author
(mohammad.awad@kustar.ac.ae)
[1]Authors are with the Khalifa University Robotics Institute, Khalifa University of Science Technology and Research, Abu Dhabi, United Arab Emirates
[2]Authors are with the BioRobotics Institue of Scuola Superiore Sant'Anna, Pontedera, Italy.
[3]Authors are with Fondazione Don Carlo Gnocchi, Florence, Italy.
[4] Authors are with Institute of Systems and Robotics and the Faculty of Science and Technology, University of Coimbra, Coimbra, Portugal
[5] Authors are with King's Collage London, UK

Variable stiffness actuators have been used in many applications, such as rehabilitation exoskeletons [24], surgical robotics [25], and haptics applications [26]. Applying compliant mechanisms to haptic devices has shown several advantages in reducing wear and weight [27, 28]. The disadvantages on the other hand lie in the increased control complexity [29]. To the author's knowledge, few haptic devices which incorporate complaint mechanisms have benefited from the resultant force from altering the compliant element. This force can be the key for force feedback in haptic devices [26]. Based on those, we suggest a new concept for haptic teleoperation application by using variable stiffness as a media to reflect force feedback. The mechanical joints of the master device are passive and transparent (zero stiffness) when no obstacle is touching/approaching the slave robot. On the other hand, the joints show resistive stiffness when the robot is halted or collided with an obstacle. The intermediate stiffness of the joints will be used to map the interaction forces encountered by the slave robot with the environment. By means of this approach, the force-feedback can be provided by the passive elements without direct energy consumption, thus allowing for smaller and lighter device to be developed.

In this paper, a new passive variable stiffness joint is presented as a bench-test for further development towards the above proposed haptic devices. The proof-of-concept design shows the ability to vary the stiffness from transparency to high values through changing the involvement of the elastic elements. The main feature of the presented concept is its simplicity, with the ability to achieve infinite range of stiffness. An infinite range of motion at zero stiffness is also achieved. The concept and the design are discussed in section II. Stiffness modeling is discussed in section III. While the physical implementation and experimental results are described in section IV. In section V, a discussion is conducted to compare this work with other related state-of-art designs. Finally, the conclusions are illustrated in section VI.

II. Concept, Mechanical Design

A. *Concept of PVSJ*

The inspiration behind the design lies in the variable lever arm mechanism but with a complete new and simpler mechanism design. In the following the concept of the pVSJ will be detailed and also compared with the other variable stiffness joints that use the lever arm mechanism.

The novelty of the pVSJ lies in the design scheme as in Fig. 1a. Two custom-made torsional springs (orange in Fig. 1a) serve the roles of both the lever and the elastic elements. The force contact point slides along the springs long arms, varying the length of the effective arm (s) of the output link where the effective arm is defined as the link between the force contact point and the joint rotation center (c). Once the output link rotates, the contact point will bend one of the two spring arms as in Fig. 1b. This will result in a contact force from the spring to the output link to balance the external torque. Change of the length of the effective arm will change the engagement of the spring with variable contact forces for the same output link rotation, indicating that the pVSJ joint can have variable stiffness. Based on this, when the force contact point coincides with the joint rotation center as in Fig. 1c the rotation of the output link will not deflect the springs since the effective arm has zero length. This results in zero joint stiffness and an unlimited rotation range. On the other hand, the highest value of stiffness is achieved by positioning the force contact point on the spring body (spring centerline n Fig. 1d). In this case, the joint can be considered as rigid with infinite stiffness (the structural stiffness of the spring body being the limit).

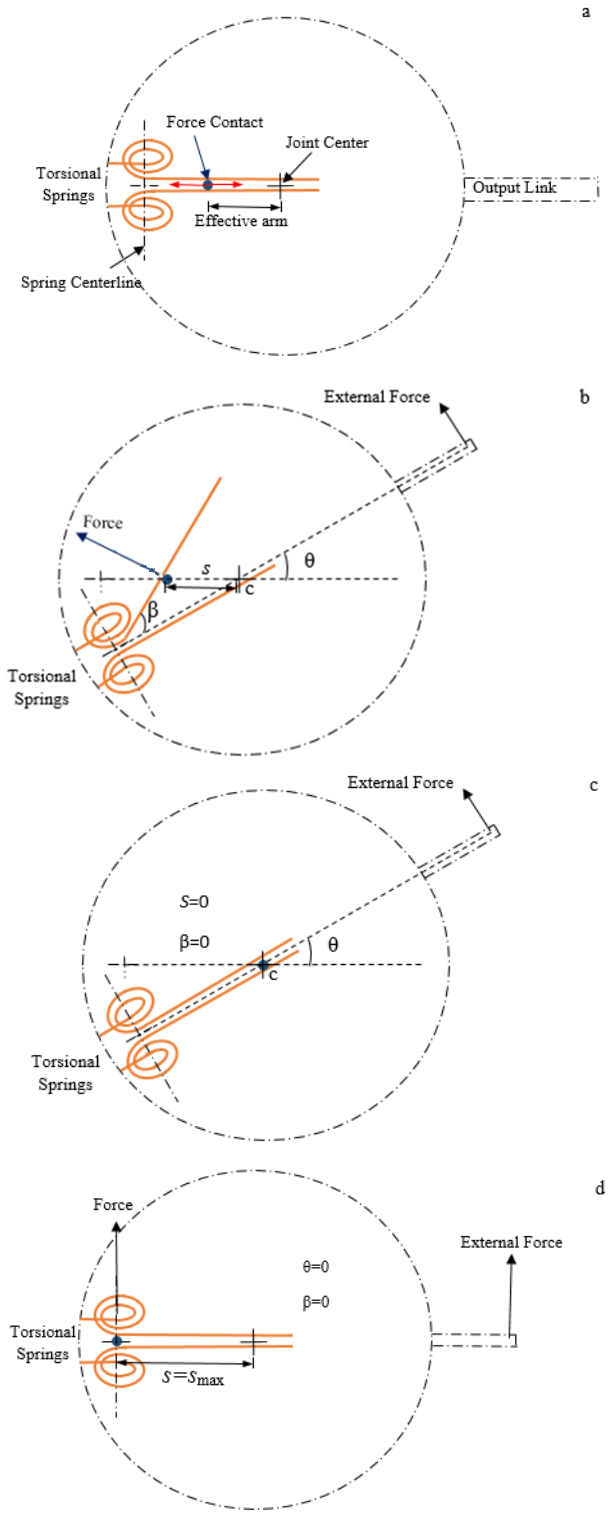

Figure 1: (a)Concept of pVSJ; the stiffness is altered by changing the length of effective arm, which will alter the involvement of the torsional spring to equalize the external torque (b) Deflection at intemediate stiffness (c) Deflection at zero stiffness (effective arm = 0). (d) maximum stiffness posture

B. *Mechanical Design of PVSJ*

Realization of the mechanical system of the pVSJ can be seen in Fig. 2. The base (fixed) consists of a linear-actuator (a DC micromotor with planetary reducer driving a lead-screw mechanism), that drives a machined plate holding the contact-force idle roller. The contact roller slides along a diameter axis of the revolute joint, crossing the main axis of rotation. The force contact position with respect to the center of rotation (effective arm) is sensed by a linear potentiometer, which is used to close the feedback loop on the linear actuator. Two custom-made torsion springs (with mirrored design) were mounted on the shaft of the joint, with their center offset from the joint axis, and the longer arm pointing along the pivot-roller sliding direction. Only one among the two spring is enrolled when an external torque loads the system. The joint deflection is sensed by an incremental optical encoder on the top of the assembly. The force/torque sensor is mounted on the far end of the output link to measure the force/torque exerted by the user.

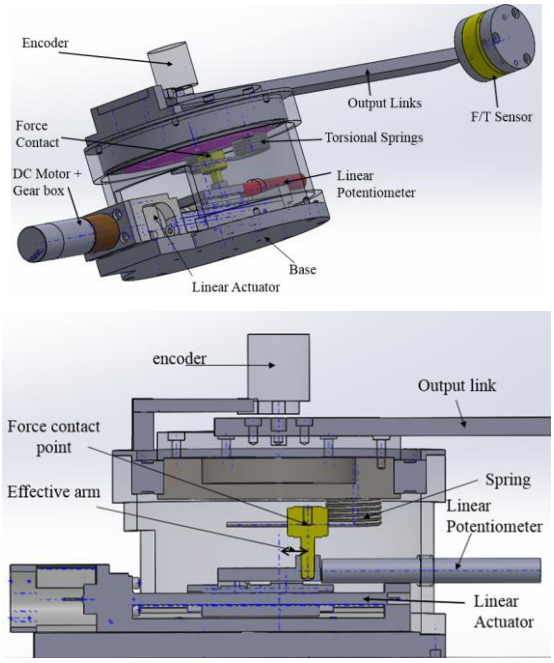

Figure 2: pVSJ, principle of operation: the linear actuator controls the position of the forced contact relative to the center of rotation (effective arm). When the length of effective arm=0, zero stiffness is achieved. When effective arm=max. full rigidity is achieved.

III. Stiffness Modeling

In order to get the model of the joint stiffness, the kinematics and the kinetics models should be presented. The kinematics is essential to estimate the deflection in the involved spring, while the kinetics model is essential to get the stiffness formula. The system works in planner coordinate (*x*, *y*) where the origin lies on the axis of rotation (*z*-axis) of the joint.

Deriving the kinematics (Fig. 3) of the joint starts by defining the effective arm (*s*), the contact roller center (C_f), the center of the torsional spring (C_s) relative to the origin (O), and the initial tangent point (B_0) between the spring's circle and its arm (at pose 0 in Fig. 3). The joint's deflection (θ) is measured from the initial position of the spring's center C_{s0} (at pose 0 in Fig. 3) to it's counterpart in the final position Cs (at pose 1 in Fig. 3).

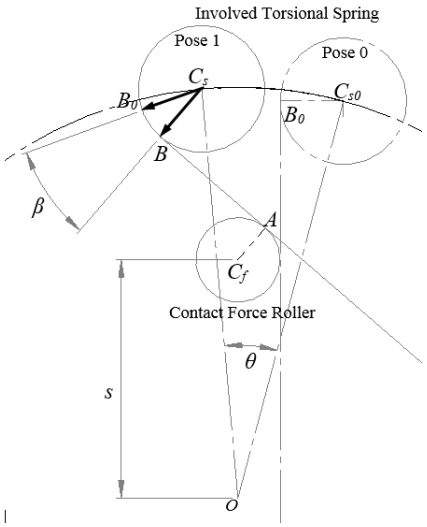

Figure 3: Kinematics Scheme for pVSJ. All points are measured from the origin (O) which is also the joint center of rotation. The initial position (pose 0) where the involved spring did not do any rotation. The final position (pose 1) is when the involved spring rotates about the origin with an angle (θ). The points are: the center of the spring at the final position (Cs), the spring's base center the initial position (Cs0) the center of the force contact (Cf), the tangent point between the deflected spring's base and its arm (B), and the point between the undeflected spring and its arm is (B0). It is noted that the displacement between the origin and center of the force contact (s) and the joint deflection angleangle (θ) are the main drivers for the deflection of the involved torsional spring (β)

In general cases when s is not zero and the output link rotates an angle θ, the arm of the involved spring will form an inner tangent line to both the spring's base circle and the force contact roller circle at points B and A respectively as in Fig. 3. In order to determine these tangential points, an algorithm to find the inner tangent of two circles (the force contact roller and the spring base) based on their center positions and radiuses was applied using the geometric relations that $\overline{(C_sB)} \perp \overline{(AB)}$ and $\overline{(AB)} \perp \overline{(AC_f)}$ (see Fig.3). The parameters (θ and s) are involved to determine the center positions of these circles as follows:

$$C_f = [0 \quad s]^T \tag{1}$$

$$C_s = \begin{bmatrix} \cos(\theta) & -\sin(\theta) \\ \sin(\theta) & \cos(\theta) \end{bmatrix} C_{s0} \tag{2}$$

where C_f, is the center of the force contact roller, C_s *is* the spring's base center at the final position (pose 1), and C_{s0} is the spring's base center at the initial position (pose 0). The deflection angle of the involved torsion spring (β) is measured from the vector starting from the spring center C_s through the initial tangent point B_0 ($\overrightarrow{\mathbf{C_sB_0}}$) to the vector starting from the spring center C_s through the new tangent point B ($\overrightarrow{\mathbf{C_sB}}$) through the following formula:

$$\beta = \arccos\left(\frac{\overrightarrow{\mathbf{C_sB_0}}}{\left\|\overrightarrow{\mathbf{C_sB_0}}\right\|} \cdot \frac{\overrightarrow{\mathbf{C_sB}}}{\left\|\overrightarrow{\mathbf{C_sB}}\right\|}\right) \tag{3}$$

From the kinematics, it can be concluded that the spring's angular deflection (β) is a function of the effective arm length

(s) and the joint angular deflection (θ). In Fig. 4, the behavior of β with respect to the change of s and θ is illustrated. It can be noted that by increasing the values of the joint's deflection angle (θ) and the effective arm length (s) , the value of the angle (β) increases from 0 to 0.7 rad with an ascenting gradient. It must be highlighted that the pVSJ joint can rotate freely at the zero stiffness case without any limitations but the operating range for non-zero joint stiffness is limited and varied as in Fig. 4. The joint rotation range is designated to be constantly 0.27rad for 0<s<18mm and then it starts decreasing in hyperbole-like curve to zero when the effective arm reaches the maximum length. This can be referred to the constraint of the spring's base geometry

After acquring all needed data from the kinematics, the kinetics model can be driven as in Fig. 5. As the joint is passive, an external torque ($\overrightarrow{\mathbf{T}_{ext}}$) is essential to obtain a defection in the joint. If the value of s equals 0, the joint will rotate freely when subjected to an external torque. When the value of s is larger than zero, one of the torsional springs will get involved to equilize the external.

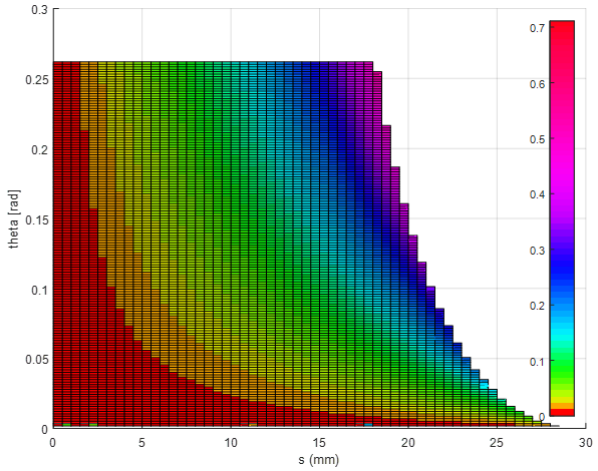

Figure 4: Behavior of the spring's angular deflection (β) (color coded) with respect of the change of force contact position (horizental-axis) and joint deflection (vertical-axis).

Exerting an external torque ($\overrightarrow{\mathbf{T}_{ext}}$) on the joint will yield a deflection (θ) for a given (s), the reaction force on the spring's base ($\overrightarrow{\mathbf{F}_s}$) has the equivelent magnitude of the force from the torsional spring's arm on the force contact with opposite direction (see Fig. 5). Hence, it can be expressed in terms of spring's Torque ($\overrightarrow{\mathbf{T}_s}$) and the spring's arm active length L_s as follows:

$$\left\|\overrightarrow{\mathbf{F}_s}\right\| = \frac{\left\|\overrightarrow{\mathbf{T}_s}\right\|}{L_s} = \frac{K_s\beta}{L_s} \tag{4}$$

where K_s is the spring's stiffness constant, at equilibirum the expression of external torque $\overrightarrow{\mathbf{T}_{ext}}$ is

$$\overrightarrow{\mathbf{T}_{ext}} = \left\|\overrightarrow{\mathbf{A}_s} \times \overrightarrow{\mathbf{F}_s}\right\| \hat{\mathbf{k}} = \left\|(\overrightarrow{\mathbf{R}_s} + \overrightarrow{\mathbf{B}_s}) \times \overrightarrow{\mathbf{F}_s}\right\| \hat{\mathbf{k}}$$

$$= \left(\frac{K_s\beta}{L_s}\left(\left\|\overrightarrow{\mathbf{R}_s}\right\| \cos(\beta) - \left\|\overrightarrow{\mathbf{B}_s}\right\| \sin(\beta)\right)\right)\hat{\mathbf{k}} \tag{5}$$

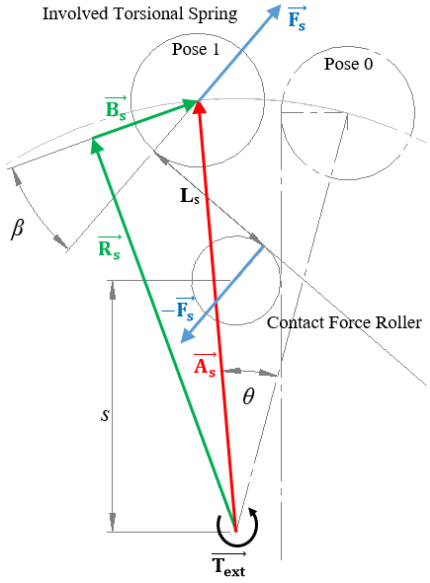

Figure 5: Kinetics schematic for pVJS: where s, $\overrightarrow{\mathbf{R}_s}$, $\overrightarrow{\mathbf{B}_s}$, $\overrightarrow{\mathbf{F}_s}$, L_s,$\overrightarrow{\mathbf{A}_s}$ $\overrightarrow{\mathbf{T}_{ext}}$ are distance from center of rotation to the center of the force contact, is the vector with a magnitude of the maximum value of s the vector with a magnitude of the distance between the effective arm line and the center of the involved spring, reaction force on the spring's base, active spring arm length the vector between the origin and $\overrightarrow{\mathbf{F}_s}$ and external torque respectively.

where $\overrightarrow{\mathbf{R}_s}$ is the vector with a magnitude of the maximum value of s. $\overrightarrow{\mathbf{B}_s}$ is the vector with a magnitude of the distance between the effective arm line and the center of the involved spring (the sum of the radius of the contact force roller and the radius of the involved torsional spring's base cylender). It's worth mentioning that $\overrightarrow{\mathbf{R}_s} \perp \overrightarrow{\mathbf{B}_s}$. The vector $\overrightarrow{\mathbf{A}_s}$ is the vector of the spring center which equals to the sum of the two vectors ($\overrightarrow{\mathbf{R}_s} + \overrightarrow{\mathbf{B}_s}$). The unit vector $\hat{\mathbf{k}}$ is in the z-th direction. It is noticed that the angle (β) lies between the two vectors $\overrightarrow{\mathbf{F}_s}$ and $\overrightarrow{\mathbf{B}_s}$. Based on the above, the joint stiffness K_θ can be expressed as follows:

$$K_\theta = \frac{\delta\left\|\overrightarrow{\mathbf{T}_{ext}}\right\|}{\delta\theta} = K_\alpha - K_\epsilon - K_\zeta \tag{6}$$

Where:

$$K_\alpha = K_s\frac{\delta\beta}{\delta\theta}\left(\frac{\left\|\overrightarrow{\mathbf{R}_s}\right\| \cos(\beta)}{L_s} - \frac{\left\|\overrightarrow{\mathbf{B}_s}\right\| \sin(\beta)}{L_s}\right) \tag{7}$$

$$K_\epsilon = K_s\beta\frac{\delta\beta}{\delta\theta}\left(\frac{\left\|\overrightarrow{\mathbf{R}_s}\right\| \sin(\beta)}{L_s} + \frac{\left\|\overrightarrow{\mathbf{B}_s}\right\| \cos(\beta)}{L_s}\right) \tag{8}$$

$$K_\zeta = K_s\beta\frac{\delta L_s}{\delta\theta}\left(\frac{\left\|\overrightarrow{\mathbf{B}_s}\right\| \sin(\beta)}{{L_s}^2} - \frac{\left\|\overrightarrow{\mathbf{R}_s}\right\| \cos(\beta)}{{L_s}^2}\right) \tag{9}$$

It can be noted from the Equations (6- 9), that the joint stiffness K_θ is directly related to the stiffness K_s of the springs. Fig. 7 illustrates this theoretically through showing the relation

of the joint stiffness versus the effective arm length (*s*) for several values of available springs.

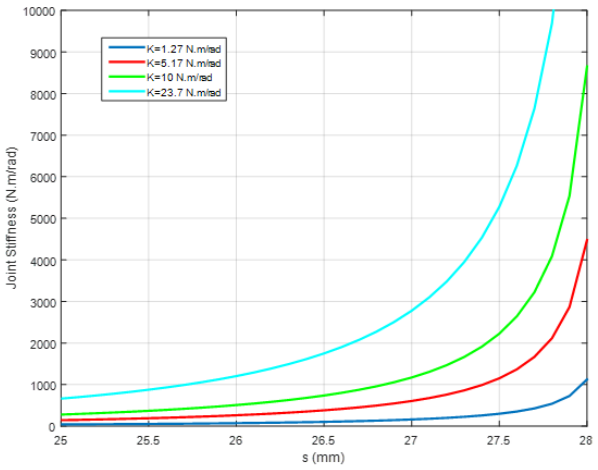

Figure8: Joint stiffness vs Force contact position for different values of spring's stiffness.

IV. Implementation of pVSJ

A custom made platform that holds the force contact roller (Misumi CFFR6-16) of diameter of 16 mm is attached to the slider of a linear actuator (Misumi LX2001-B1-E2040-10). To control the effective arm length represented by the position of the contact roller a brushless DC-servomotor (Faulhaber 2232-BX4-CXD-DFF) with a 51:1 planetary gearbox (Faulhaber 22F1) is used to connect to the lead screw shaft in the linear actuator. Two torsional springs (stainless streel A316, OD: 20 mm, active coils: 4, RD: 2.5mm, L1: 50 mm, L2= 15 mm) are fixed on the 90 mm diameter shaft of the output link. The centers of the springs have the displacements from the origin of (-18 mm, 30 mm) and (18 mm, 30 mm) respectively. This arrangement tightens the long arms of the springs on the force contact (see Fig. 6). The chassis is built from Aluminum Alloy.

Three sensors were used in the pVSJ prototype. The incremental optical encoder (Kubler 05.2420) is used to measure the joint angular deflection (θ). A linear potentiometer (Curtis Wright SLS095) is used to measure the force contact's position with respect to the center of rotation (*s*). The force/torque sensor (ATI F/T Mini-40) is used to measure the external force on the output link. National Instrument FPGA (C-RIO 9014) with National Instrument LabView® software was used for real-time control and data monitoring. Detailed design specifications can be seen in Table 1.

To validate the stiffness model, some experimental tests were conducted. By changing the values of the effective arm length (*s*), the experimental results have proven the system behaves similar to the proposed model (see Fig.8). It can be noted that the stiffness changes very slowly when the effective arm length is from 0 to 25 mm. Then the values of the stiffness boost to very high levels in the last 5 mm. This can be interpreted as the values of L_s in Equations (6-9) becomes very small. On the same hand, at *s*=30 mm, the force contact reaches the space between the two spring bases which behave as a rigid stop.

To evaluate the ability of the pVSJ to change the stiffness, the joint deflection is measured through the optical encoder, and the external torque is measured through the Force/Torque sensor. An experiment was conducted by placing the contact roller in different positions, corresponding to different values of *s*. In each of these settings, the external torque versus the joint angular deflection for several values of *s* was recorded and the result are illustrated in Fig. 9. It is shown that for small values of *s*, it requires low external torque for a wide span of angular deflection. As the value of *s* increases the required external force increases for the same value of joint deflection. The span of angular deflection gets narrower by the increment of the value of *s*. This can be referred to the increment of the stiffness and the decrement of the workspace. Analyzing the experimental results for the operating range (see Fig. 10). The experimental results slightly deviates below the simulation results in the range ($18 < s < 20$ mm). This can be referred to the thickness of the spring arm, which was not included in the simulation model. The experimental results also deviates with maximum 0.02 rad above the simulation results in the range ($23\text{mm} < s < 30\text{mm}$). This can be referred to the presence of backlash.

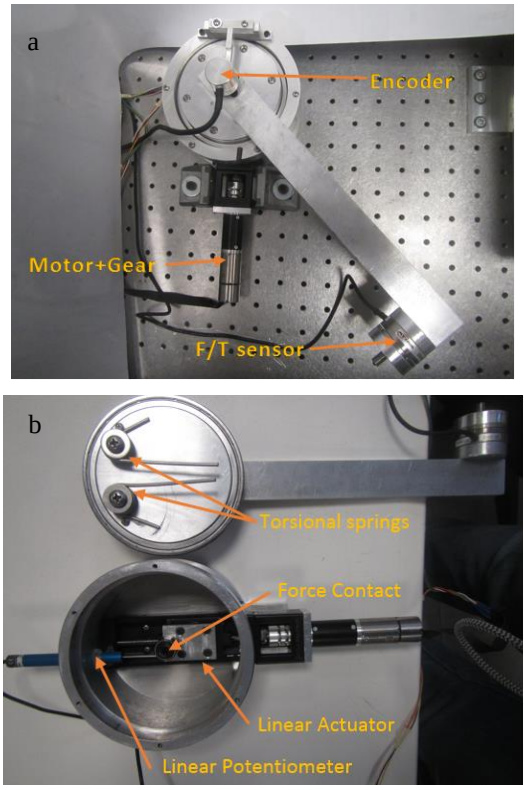

Figure6: a) pVSJ , b) disassembled pVSJ

TABLE I. pVSJ Design Parameters

Specification	Value	Units
Force contact range of motion	0 – 0.03	m
Force Contact Diameter	0.016	m
Desired range of motion for zero stiffness joint	-π/2 to π/2	rad
Desired range of motion for non-zero stiffness joint	-0.27-0.27	rad
Spring Stiffnesss Constant	1.27	N.m/rad
Maximum applied torque	15.2	N.m

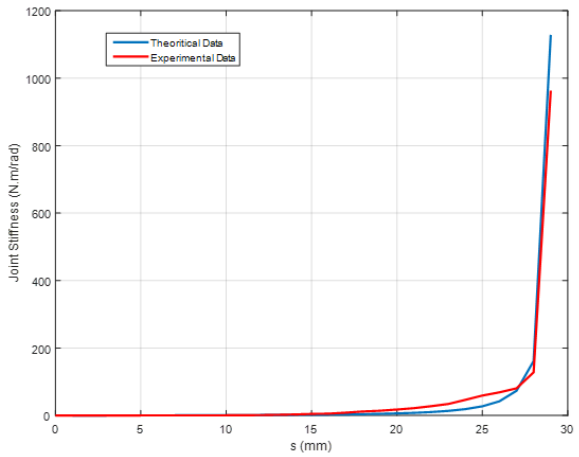

Figure 8: Model (Theoretical) of the stiffness values (blue), compared with Experimental data (red) subjected to the change of values of s.

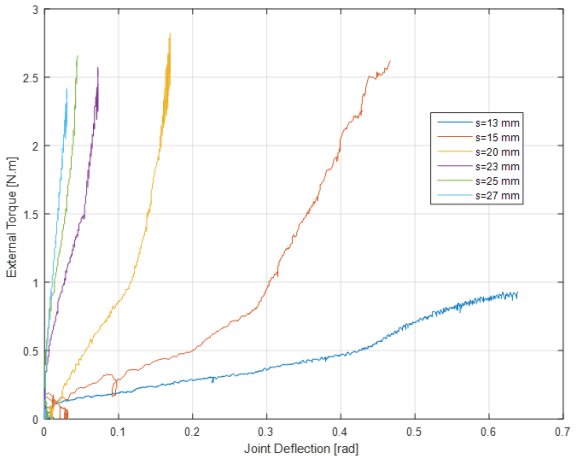

Figure 9: External Torque vs Joint angular deflection for several values of *s*.

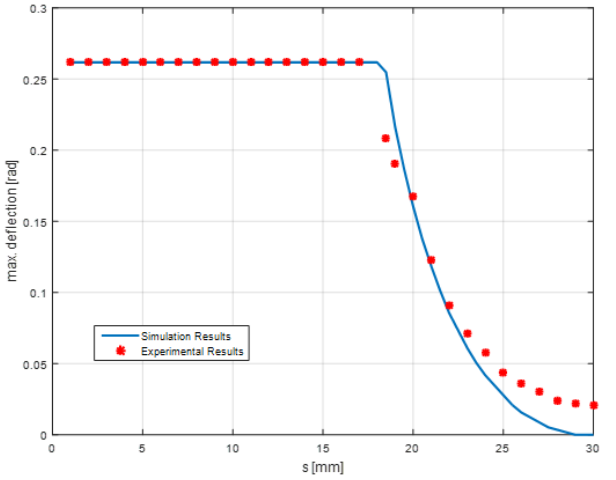

Figure 10: Operating range for non-zero stiffness joint ; theoretical values (blue), exprimental data (red)

V. Discussion

The pVSJ belongs to the category of variable-stiffness joints that alter their stiffness through changing the length of effective arm. Thanks to its design, the pVSJ can achieve zero to infinite stiffness with unlimited rotation in the zero stiffness case applying simple, cost-effective, easily manufactured and light-weighted components. Tuning spring effective arm was also used in the AWAS [18] but it has limited stiffness range and limited rotation range for all cases. Infinite stiffness range was achieved in AWAS-II [19] by using the concept of tuning the pivot position and a compact version, compact-VSA [20] , was also developed using a rack-pinion system to control the pivot position. Based on the same model, an epicyclic gearing system was proposed in [22] to linearly position the pivot. But all those designs have limited range of rotation motion at the zero stiffness configuration due to the mechanical constraints while a large range of rotation at the zero stiffness is preferred in teleoperation as it is used when the robot does not touch the environment

The infinite stiffness range and unlimited range of motion at zero stiffness was also achieved in the variable stiffness mechanism presented in [30]. In this mechanism, the stiffness is altered through changing the position of the supports of two leaf springs. This is realized through hypocycloid gearing mechanism which allows direct drive of the supports by the motor. However, this realization introduces back-drivability. On the other hand, the pVSJ presents a different simple implementation for altering the spring leverage, by driving the position of the force contact through a linear actuator (motor, gearbox and a leadscrew). This realization introduces velocity saturation due to the limitation in the mechanical properties of the linear actuator. This reduces the maximum rate of change in stiffness with time. However, the leadscrew is self-locking when the coefficient of friction is greater than the lead angle [32]. Moreover, using the linear torsional springs in the pVSJ eases the stiffness modeling as well as being a cost-effective option and easily manufactured. On the other hand, using the leaf springs in [30] allows the designer of obtaining a desired stiffness vs angle curve based on the design requirement. However, modeling the stiffness of the mechanism will include the non-linear Euler–Bernoulli model of the leaf spring.

VI. Conclusions

In this paper, the mechanical design, physical model and system characterization of the passive variable stiffness joint (pVSJ) were presented. The concept of varying the stiffness through altering the involvement of coil torsional springs presented here is novel. The concept is realized through a position-controlled force contact which changes the length of the effective arm representing the engagement of the springs. A physical model is presented and verified by the experimental results, which showed that the joint is capable to achieve infinite range of stiffness with infinite range of motion at the zero stiffness value.

In the future, a design underlying on the same concept will be realized, but focusing on attaining a much lower weight, a faster change for the contact roller position. These intended developments to achieve better results when applying for wearable haptic devices. The author intends to investigate the

non-linear effect of the torsional spring's arm deflection on the stiffness performance, including more parameters in the simulation model.

REFERENCES

[1] N. G. Tsagarakis, I. Sardellitti, and D. G. Caldwell, "A new variable stiffness actuator (CompAct-VSA): Design and modelling," in Proc. IEEE/RSJ Int. Conf. Intell. Robots Syst., 2011, pp. 378–383.

[2] N. Hogan, "Impedance control: an approach to manipulation: part III - applications, Journal of Dynamic Systems, Measurement, and Control 107 (2) (1985) 17.

[3] R. Bischoff, J. Kurth, G. Schreiber, R. Koeppe, A. Albu-Schäffer, A. Beyer, O. Eiberger, S. Haddadin, A. Stemmer, G. Grunwald, et al., The KUKA-DLR lightweight robot arm-a new reference platform for robotics research and manufacturing, in: 6th German Conference on Robotics, ROBOTIK, VDE, 2010

[4] A. Albu-Schaffer, S. Haddadin, C. Ott, A. Stemmer, T. Wimbock, G. Hirzinger, The DLR lightweight robot: design and control concepts for robots in human environments, Industrial Robot: An International Journal 34 (5) (2007) 376–385.

[5] Pratt, G., and Williamson, M., 1995, "Series Elastic Actuators," Proceedings of the 1995 IEEE/RSJ International Conference on Intelligent Robots and Systems, Vol. 1, pp. 399–406.

[6] Tonietti, G., Schiavi, R., and Bicchi, A., 2005, "Design and Control of a Variable Stiffness Actuator for Safe and Fast Physical Human/Robot Interaction," International Conference on Robotics and Automation, Barcelona, Spain.

[7] Wolf, S., and Hirzinger, G., 2008, "A New Variable Stiffness Design: Matching Requirements of the Next Robot Generation," IEEE International Conference on Robotics and Automation, pp. 1741–1746.

[8] Tsagarakis, N. G., Laffranchi, M., Vanderborght, B., and Caldwell, D. G., 2009, "A Compact Soft Actuator for Small Scale Robotic Systems," International Conference on Robotics and Automation, Kobe, Japan.

[9] Curran, S., Knox, B. T., Schmiedeler, J. P., and Orin, D. E., 2009, "Design of Series-Elastic Actuators for Dynamic Robots with Articulated Legs," ASME J. Mech. Rob., 1(1), p. 011006.

[10] T. Sugar, A novel selective compliant actuator, Mechatronics 12 (9) (2002) 1157–1171

[11] D. Gan, N. G. Tsagarakis, J. Dai, D. Caldwell, L. Seneviratne, Stiffness Design for a Spatial Three Degrees of Freedom Serial Compliant Manipulator Based on Impact Configuration Decomposition, Journal of Mechanisms and Robotics, 2013

[12] M. Zinn, O. Khatib, B. Roth, J. Salisbury, Playing it safe [human-friendly robots], IEEE Robotics & Automation Magazine 11 (2) (2004) 12–21

[13] R. Schiavi, G. Grioli, S. Sen, A. Bicchi, VSA-II: a novel prototype of variable stiffness actuator for safe and performing robots interacting with humans, in: IEEE International Conference on Robotics and Automation, ICRA 2008, 2008, pp. 2171–2176

[14] Hurst, Jonathan W, Chestnutt, Joel, & Rizzi, Alfred. 2004. An Actuator with Mechanically Adjustable Series Compliance. April.

[15] Migliore, Shane A., Brown, Edgar A., & DeWeerth, Stephen P. 2005 (April). Biologically Inspired Joint Stiffness Control. Pages 4519–4524 of: IEEE International Conference on Robotics and Automation (ICRA 2005).

[16] R. Van Ham, B. Vanderborght, M. Van Damme, B. Verrelst, D. Lefeber, MACCEPA, the mechanically adjustable compliance and controllable equilibrium position actuator: design and implementation in a biped robot, Robotics and Autonomous Systems 55 (10) (2007) 761–768.

[17] B. Vanderborght, N. Tsagarakis, R. Van Ham, I. Thorson, D. Caldwell, Maccepa 2.0: compliant actuator used for energy efficient hopping robot chobino1d, Autonomous Robots (2009) 1–11.

[18] A. Jafari, N. Tsagarakis, B. Vanderborght, and darwin Caldwell, "Awas: a novel actuator with adjustable stiffness," is in the Proceeding of IEEE/RSJ International Conference on Intelligent Robots and Systems (IROS), 2010.

[19] Amir Jafari, Nikos G. Tsagarakis and Darwin G. Caldwell. "AwAS-II: A New Actuator with Adjustable Stiffness based on the Novel Principle of Adaptable Pivot point and Variable Lever ratio" IEEE International Conference on Robotics and Automation, 2011, pp.4638-4643.

[20] N. G. Tsagarakis, I. Sardellitti, and D. G. Caldwell, "A new variable stiffness actuator (CompAct-VSA): Design and modelling," in Proc. IEEE/RSJ Int. Conf. Intell. Robots Syst., 2011, pp. 378–383.

[21] L. C. Visser, R. Carloni, and S. Stramigioli, "Energy efficient variable stiffness actuators," IEEE Trans. Robot., vol. 27, no. 5, pp. 865–875, Oct. 2011.

[22] M. Fumagalli, E. Barrett, S. Stramigioli, and R. Carloni, "The mVSA-UT: A miniaturized differential mechanism for a continuous rotational variable stiffness actuator," in Proc. IEEE/EMBS Int.Conf. Biomed. Robot. Biomechatron., 2012, pp. 1943–1948.

[23] Wolf, S., Eiberger, O., and Hirzinger, G., 2011. "The DLR FSJ: Energy based design of a variable stiffness joint." In 2011 IEEE International Conference on Robotics and Automation, DLR - German Aerospace Center, Institute of Robotics and Mechatronics, D-82234 Wessling, Germany, Ieee, pp. 5082–5089. 4 55

[24] T. Bacek, R. Unal, M. Moltedo, K. Junius, H. Cuypers, B. Vanderborght, D. Lefeber, "Conceptual Design of a Novel Variable Stiffness Actuator for Use in Lower Limb Exoskeletons" IEEE International Conference on Rehabilitation Robotics, 2015, pp. 583-588

[25] A. Jiang, G. Xynogalas, P. Dasgupta, K. Althoefer, and T. Nanayakkara, "Design of a variable stiffness flexible manipulator with composite granular jamming and membrane coupling," IEEE/RSJ International Conference on Intelligent Robots and Systems (IROS 2012), Vilamoura, Portugal, 2012.

[26] Hawks, Jeffrey C., "A Variable-Stiffness Compliant Mechanism for Stiffness-Controlled Haptic Interfaces" (2014). All Theses and Dissertations. Paper 4356.

[27] Lu, K.,. "Design and Application of Compliant Mechanisms for Surgical Tools." Journal of Biomechanical Engineering, 127(6), July, 2005 p. 981. 5

[28] Awtar, S., Trutna, T. T., Nielsen, J. M., Abani, R., and Geiger, J.,. "FlexDex: A Minimally Invasive Surgical Tool With Enhanced Dexterity and Intuitive Control." Journal of Medical Devices, 4(3), 2010 p. 035003. 5

[29] Gillespie, R. B., Shin, T., Huang, F., and Trease, B., 2008. "Automated Characterization and Compensation for a Compliant Mechanism Haptic Device." IEEE/ASME Transactions on Mechatronics, 13(1), Feb., pp. 136–146. 5

[30] S. Groothuis , R. Carloni , S. Stramigioli, A Novel Variable Stiffness Mechanism Capable of an Infinite Stiffness Range and Unlimited Decoupled Output Motion, Actuators 2014, 3, 107-123

[31] B. Vanderborght et al. "Variable impedance actuators: A review", Robotics and Autonomous Systems 61 (2013) 1601–1614

[32] V. B Bhandari , "Design of Machine Elements" 3rd Edition, McGraw-Hill, 2010